

## **A High-Precision Position-Based Calibration Table as the Reference for Angular Accelerometer Calibration Experiment**

*Dyah Jatiningrum*

*Delft University of Technology*

*PhD Student*

*Kluyverweg 1, Delft, 2629HS, The Netherlands*

*D.Jatiningrum@tudelft.nl*

*Andries Muis #1 (Delft University of Technology), Coen de Visser #2 (Delft University of Technology),*

*Rene van Paassen #3 (Delft University of Technology), Max Mulder #4 (Delft University of Technology)*

### **ABSTRACT**

With the role of angular accelerometers in future fault-tolerant flight control systems, an in-depth evaluation of their performance then becomes a critical issue from the perspective of control system design. In this paper, a position-based calibration table is utilized to provide a sufficiently accurate angular acceleration reference in the dynamic angular calibration. However, the angular accelerometer measured data contains a high noise level when transmitted through the slip rings. To tackle this issue, a customized sensor Data Acquisition System (DAS) is designed. It is mounted on the turn-table top and has a direct access to the angular accelerometer data channel. To synchronize sensor and table data, two auxiliary signals are generated by the sensor DAS computer to help in the post measurement processing. The first signal is a regular pulse of  $100\text{ Hz}$ , which is suitable to align sensor and table data. The second signal is a step function which acts as a data log trigger for the calibration table, as well as a marker of the record starting point. This approach results in a lower angular accelerometer noise level, below the specified limit of  $3\text{ mV}$ . The  $Error_{RMS}$  is  $0.00195\sigma_{n1}$ , which after being calculated with the measurement results, evidently falls below the Gaussian probability density function specified by the standard of  $\pm 5.672$ . As a result, the customized setup enables a commercially available calibration table to serve as the reference for angular accelerometer calibration experiments.

### **Nomenclature**

*DAS* Data Acquisition System

*FP* Freeze Pulse

*F<sub>s</sub>* sampling frequency

*IMU* Inertial Measurement Unit

*INS* Inertial Navigation System

*S* Continuous sinusoidal signal

*S<sub>I</sub>* Simulated sinusoidal signal

*S<sub>das</sub>* Measured sinusoidal signal in the sensor DAS

*S<sub>tab</sub>* Measured sinusoidal signal in the calibration table control center

*T<sub>k-1</sub>* time interval between the freeze pulse and the start of the next Servo Frame

*T<sub>k</sub>* time interval of the next Servo Frame

*t<sub>start</sub>* table data time correction towards the freeze pulse

## 1 INTRODUCTION

PROVIDING a sufficiently accurate angular acceleration reference for angular accelerometers calibration is not trivial and has become one of the main concerns in *dynamic* angular sensor calibration. Part of it is due to the present emphasis on gyroscopic sensors, in which *static* accuracy is the primary factor.[1] The available test equipment consequently follows this pattern. Usually, the equipment does have a dynamic capability, but it is much less accurate than when it performs static operations. Furthermore, these motion simulator bases often bring unwanted dynamics, non-linearity, transport delays, etc. making it difficult to separate sensor issues from test equipment problems.[2, 3]

Angular accelerometers are novel inertial sensors that may play a significant role in future fault-tolerant flight control systems. Recently, researchers are focusing on developing fault tolerant flight control systems that require angular acceleration feedback, which is currently obtained by differentiating the rate gyro signals. For example, the Incremental Nonlinear Dynamic Inversion technique is a state-of-the-art fault tolerant control system that is robust to on-board model mismatches. It greatly increases the performance of the system compared to conventional nonlinear dynamic inversion.[4] Other studies discuss a Sensor-based Backstepping approach implementation into fault-tolerant flight control systems.[5, 6] The performance of both control approaches are expected to be significantly improved when using angular accelerometers instead of differentiated gyro signals.

At present, angular accelerometers are applied in specific fields such as missile control, pointing camera platforms, gun sights, and laser mounts.<sup>1</sup> However, it is not standard in current commercial aircraft Inertial Navigation Systems (INS) applications. Angular accelerometers directly measure angular acceleration, in contrast to the indirect approaches. There are three noted indirect approaches[7]: (1) differentiation based on analog or digital post-processing of available position or angular velocity signals, (2) predictive post-filtering, and (3) linear state observing. Another recognized approach to measure angular acceleration is to use a pair of linear accelerometers to provide angular acceleration along with translational accelerations.[8, 9]

In-depth evaluation of the angular accelerometers performance before it is integrated in the fault-tolerant flight control system then becomes a critical issue in the perspective of control system design. To evaluate an inertial sensor performance, a notion of the "true" motion is crucial. Besides exciting the sensors, the input motion should possess the required quality as a reference in a calibration. Turntable systems, referred to in this paper as calibration tables, are widely used to produce the appropriate input motion sequence. Its mounting platform's orientation can be single-axis, or two to three axis degree-of-freedom.

In the case of linear accelerometers, the angular-velocity-sensitive and angular-acceleration-sensitive coefficients in the performance model can be calibrated using high-rate rotations on a rate table.[10] Thus, a commercially available calibration table is suitable to perform the calibration. For angular accelerometers, however, the calibration procedure is not as straightforward. One of the main reasons is due to the current table estimated angular acceleration insufficiently serve as a reference. The calibration table uses indirect acceleration measuring techniques based on analog or digital post-processing of available position signal and afterwards, a band-limited differentiators to construct the acceleration signal.

Another surfacing issue is that the measured angular accelerometer signal becomes very noisy when relayed through the slip rings, even with the addition of a pre-sample filter to eliminate the high frequencies noise. Slip rings enable the transfer of electric power or signal circuits across a rotating surface, which is a common feature in today's calibration table. It simplifies the measurement set-up and allows the calibration table clock to bypass and coordinate the sampling in the sensor data acquisition system (DAS). In this particular case however, a modified set-up most likely needs to be arranged to ensure a good quality of obtained angular accelerometers data.

<sup>1</sup>A Guide to Accelerometer Selection. <http://www.cfxtech.com/rhow.htm>

This paper presents the possible solution on how to carry out the angular accelerometers calibration experiment by utilizing a position-based calibration table. To address the slip ring noise issue, a new measurement set-up with a direct sensor DAS is developed. Although the new configuration successfully meets the specified angular accelerometer noise level, no direct sampling clock connection is possible. The measured data therefore requires synchronization, which in this new set-up is achieved by generating two auxiliary signals. The first signal is a regular pulse of  $100\text{ Hz}$ , which is sent continuously from the sensor DAS computer to the calibration table. It is suitable to align sensor and table data by means of orientation on its rising edge. The second signal is a step function, which also generated and sent from the sensor DAS computer. It serves as a data log trigger for the calibration table, as well as a marker of the record starting point.

The paper is structured as follows. In Section 2, the calibration background is introduced. Subsequently, the system description, comprised of measurement set-up and the development of a customized set-up for angular accelerometer calibration, the data synchronization method, and test procedures are provided in Section 3 on the next page. The investigation on the test set-up is discussed in Section 4 on page 8. Concluding remarks are given in Section 5 on page 13.

## 2 INERTIAL SENSOR CALIBRATION USING TURN-TABLE

To obtain a correct sensor measurement, it is necessary to measure the output of a sensor in response to an accurately known input. This process is known as calibration, and the devices that produce these inputs are called calibration standards. There are two types of calibrations: static calibration and dynamic calibration. Static calibration is performed when time is not relevant in the measurement. It relates to the properties of the system after all transient effects have settled to their final or steady state. On the other hand, dynamic calibration is required when time is relevant to the measurement. This type of calibration attends to the properties of the system transient response to an input.

For aircraft inertial sensors, the above-mentioned calibration also applies. Nevertheless, testing and calibration methods need to reflect the type of application, since the required performance varies widely in each. One of the purposes of testing an inertial sensor is to evaluate the mathematical representation of sensor behaviour, so that the performance of a sensor can be predicted for particular circumstances, and eventually enhancing its accuracy.

Using a turn-table is a well known and widely employed calibration method. The three-axis variant is especially capable of simulating the three degrees-of-freedom motion of an aircraft and thus, applicable as the calibration standards for inertial sensors. The calibration-table-generated motion has been used to produce not only excitation for different types of inertial sensors such as linear accelerometers [11, 12] and gyroscopes [13, 14], but also for groups of sensors in for instance Inertial Measurement Units (IMU)[15, 16, 17].

The calibration table operated by Control and Simulation Section, Faculty of Aerospace Engineering – TU Delft, is the calibration standard in this paper. It is capable of simulating or accurately reproduce roll, pitch and

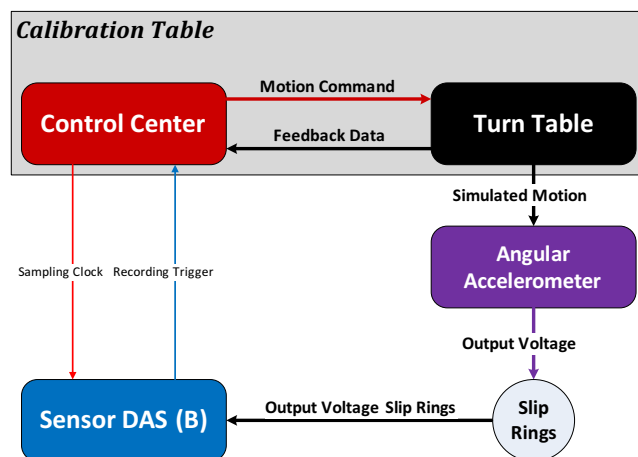


**Figure 1: Basic diagram**

yaw motion in the laboratory environment for inertial sensors calibration. As a position-based calibration table, it offers excellent instantaneous rate stability and precise and stable positioning.

The basic diagram of an angular accelerometer measurement using the calibration table is shown in Figure 1 on the preceding page. The calibration table system consists of two subsystems: the control center and the turn-table, whereas the sensor system includes three subsystems: the angular accelerometer, slip rings and DAS. The control center accurately steer the turn-table motion as well as provides estimates for the angular rate and acceleration signal. The device has a 2-axis, high-precision, position-based turn-table. As a position-based calibration table, it provides an extremely-accurate angular displacement measurement. The angular accelerometer can be mounted and secured on the turn-table inner axis rotating plate, whereas slip rings provides power and data channels connection to the DAS instrumentation. The slip rings are an electromechanical device that is an integrated part of the turn-table, it allows the transmission of power and electrical signals from a stationary to a rotating structure. Additionally, two direct connections between the control center and DAS computer are established to coordinate the data sampling for both the calibration table and angular accelerometer, and trigger to start the recording process, such that the initial data point and duration are synchronized.

### 3 ANGULAR ACCELEROMETER CUSTOMIZED MEASUREMENT SET-UP TEST

The following subsections are describing the measurement set-up, the data synchronization and the experiment procedure for the case of an angular accelerometer.

#### 3.1 Customized Measurement Set-up

In the static measurement evaluation using the setup in Figure 1 on the previous page, it was found that the measured angular accelerometer is perturbed by a noise signal that exceeds the  $3\text{ mVRMS}$  specification<sup>2</sup>. The angular accelerometer was then observed in a series of static measurements evaluation to identify the source of disturbance. The configurations tested in this regard involved some power setting and locking mechanism of the calibration table as it was suspected that they might have some influence in the measurement. The following items are the setting for the evaluation measurements.

1. Normal measurement configuration
2. Axis motor lock off
3. Calibration table power off and axis motor lock off
4. Sensor power off, calibration table power off, and axis motor lock off

Even with both the equipment and sensor off as in item 4, the noise level in the angular accelerometer data channel reached  $14\text{ mV}$ . It can be seen that the slip rings contribute a  $14\text{ mV}$  noise into the sensor measurement and in this case, resulted in a much higher angular accelerometer noise.

To confirm the hypothesis, another measurement was conducted with a direct connection between the angular accelerometer and DAS unit on a stable surface. The measurement returns a  $0.992\text{ mV}$  noise level of the angular accelerometer. Accordingly, it can be safely assumed that in order to obtain a meaningful angular accelerometer data, the measurement should not be performed through the slip rings. This means that modifying the basic measurement setup is necessary.

The challenge of the modification is how to record angular accelerometer data directly without the use of slip rings, as depicted in Figure 2(a) on the next page. An immediate cable connection from the sensor to the basic DAS would be ideal, nevertheless it is a potential hazard in dynamic excitation and inevitably limits the motion simulator to only one axis of rotation.

<sup>2</sup>[www.crlsensors.com](http://www.crlsensors.com)

A viable solution is achieved by placing a compact, customized DAS on top of the turn-table plate together with the sensor, as seen in Figure 2(b). The slip rings provide power to both the sensor and DAS, but the angular accelerometer data channels are connected to the DAS computer. Additionally, a pre-sample filter is added before the DAS to eliminate the high-frequency noise. The mounted DAS computer can be accessed via a wifi connection from a nearby desktop.

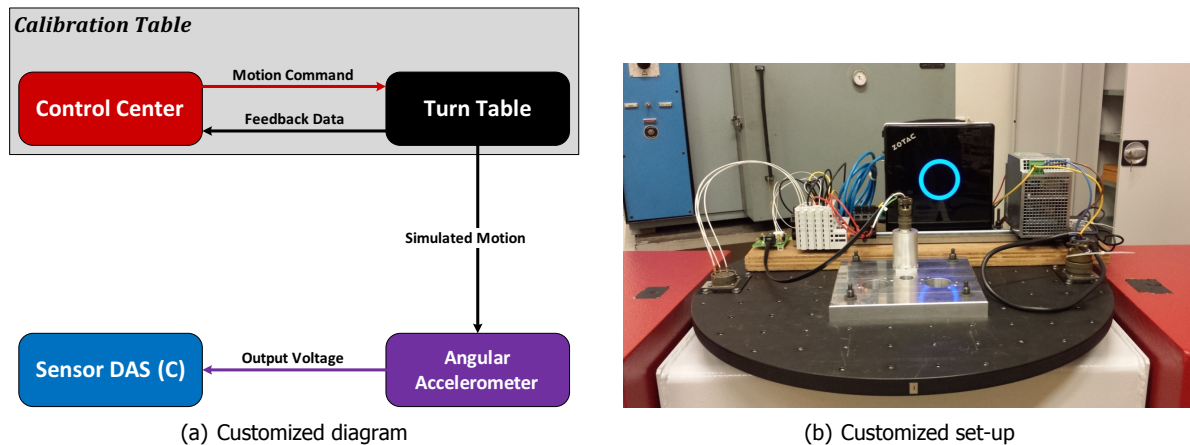


**Figure 2: Customized diagram and Customized set-up**

This customized set-up is unable to accommodate the common clock connection from the calibration table control center, which leads to a potential timing error in the acquisition. Further data post-processing is needed to match angular accelerometer and calibration table data such that the comparison can be justified. Before being able to do so, first we need to resolve how the synchronization will be performed.

The key to synchronization is to have a common marker that can be used to align the two data sets from different sources. This can be implemented with the help of a regular pulse, where the rising edge is used as an orientation. Because the sensor DAS starts to record once the acquisition application has commenced, but the calibration table control center is not, a step signal is generated as a trigger for the calibration table and to mark the beginning of the recording. The synchronization procedure is explained in Section 3.2 and a basic test using an external stable signal is described in Section 3.3 on page 8.

### 3.2 Synchronization Procedure using Freeze Pulse Marker

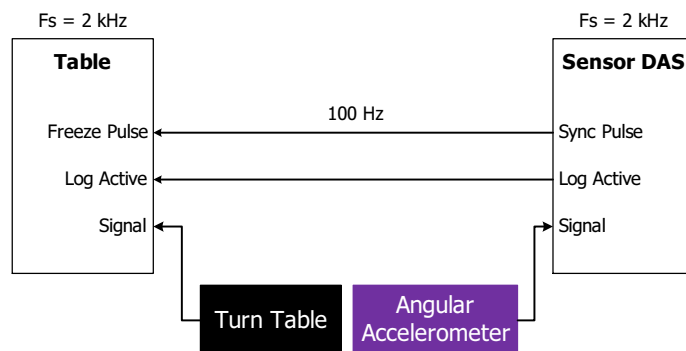


**Figure 3: Measurement set-up with sync pulse**

Each computer has a circuit for keeping track of time which is usually referred to as *clock*, usually in a form of a precisely machined quartz crystal. In ideal situation, the clock or timer oscillates at a well-defined frequency. Although the frequency runs is usually fairly stable, it is impossible to guarantee that the crystals in different computers all run at exactly the same frequency. When a system has  $n$  computers, all  $n$  crystal clocks will run at slightly different rates, causing them to gradually get out of sync and give different values when being read out.

Clock synchronization is possible and need not be absolute[18]. What usually matters is not that all processes agree on exactly what time it is, but rather, that they agree on the order in which events occur or relative times. This statement applies in this paper, which is not a *real-time* situation, and therefore will attempted to employ a logical clock synchronization rather than physical clock.

The common marker or sync pulse, is generated in the form of regular pulse with  $100\text{ Hz}$  frequency in the sensor DAS computer. Simultaneously, a step signal to activate the recording function is generated in the sensor DAS computer with logic of 0 before recording and 1 for the start of the recording and the rest. Both signals are sent to the calibration table control center by means of digital input-output interface. The sampling frequency  $F_s$  for both control center and sensor DAS are  $2\text{ kHz}$ . Figure 3 on the previous page illustrates the schematic of this connection.

The received sync pulse signal is recognized as a freeze pulse by the control center. This feature is originally used to generate a set of motion variables that are accurate in time to an external reference signal. For this study, the concept is employed to align the Sensor DAS computer and control center clocks, and furthermore the data. To aid the synchronization, several variables of interest needs to be recorded in the control center:

- Sync pulse from sensor DAS computer, a  $100\text{ Hz}$  pulse.
- Trigger signal from sensor DAS computer, marking the beginning of the recording.
- Freeze pulse latched.
- Freeze pulse latched time in counts.
- Freeze pulse latched time in seconds.

The key to understand the operation is to understand when the various events involved actually happen. The estimated variable is the output of the observer and since it is a Predictive Estimator, its output is valid at the end of the cycle where the computations take place. The data logger then collects information at the end of the servo cycle. The freeze pulse received during a cycle is time stamped immediately but it is processed only until the next cycle, as shown in Figure 4 timing diagram<sup>3</sup>.

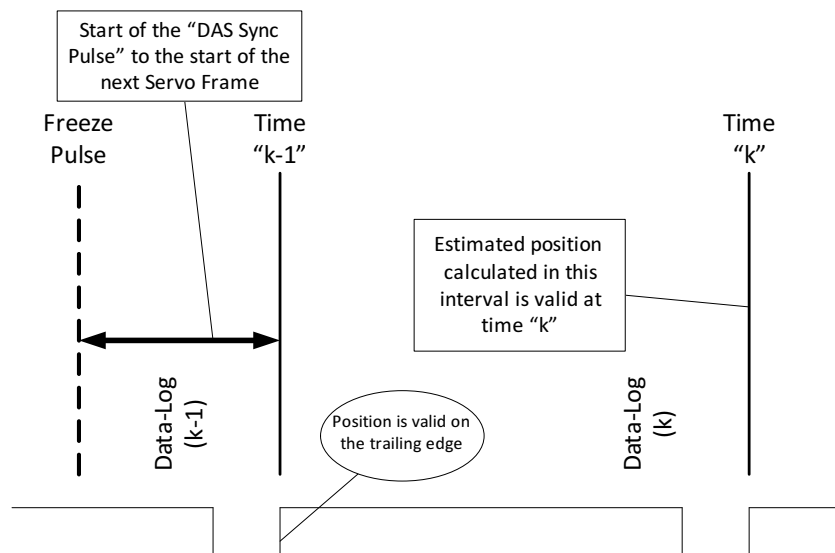


**Figure 4: Freeze Pulse Timing Diagram**

<sup>3</sup>Freeze Pulse Feature on the ACUTROL® 3000, White Paper



Then the table data needs to be corrected for  $t_{start}$  to match the freeze pulse.

$$t_{start} = T_{k-1} + T_k \quad (1)$$

Where  $T_{k-1}$  is the time interval between the the freeze pulse and the start of the next Servo Frame, and  $T_k$  is the time interval of the next Servo Frame

To find the first freeze pulse in the record, Freeze Pulse (FP) Latched's active (1) and non-active (0) status is used. A new logic variable is constructed where FP Latched is equal to 1 and Log Active also equal to 1. The data log capture showing the transition of a freeze pulse occurrence is shown in Table 1. The highlighted parts are the first FP Latched where logging is active and the FP Latch Time is corresponding to this.

Another logic vector is created from FP Logic, where the data is shifted one sample backward<sup>4</sup> and TRUE only at the start of the pulse. This in turn correlates to the actual starting time of the first recorded pulse.

The Table FP Time itself is the difference between Table Time and FP Latch Time. Since the FP Latch Time is the same in one pulse period<sup>5</sup>, it can be simplified by extracting FP Latch Time using FP Logic\*. Consequently, the Table Time need to be adjusted, this can be done by extracting using FP Logic\*. Therefore, the Table FP time is 20 times shorter than the original total data points. Table 1 provides an application example of the synchronization procedure to the measurement data.

Finding Freeze Pulse on the DAS Time is performed using a similar method. However, the resulting DAS FP Time is longer than FP time because its record starts earlier and stops later.

**Table 1: Creating FP Logic from FP Latched**

FP Latched	FP Latched Time	FP Logic	FP Logic*	Table Time	Remarks
0	0.00024	False	False	246.0853	Time (n-2): Data logger takes a snapshot right before the time "n-2" as shown on the diagram in Fig. 4.
0	0.00024	False	True	246.0858	Time (n-1): Pulse took place between (n-2) and (n-1). Time between the sync pulse and "n-1" sample are measured, but the real-time software is totally unaware of this event at this time.
1	0.00023	True	False	246.0863	Time (n): real-time software is now aware of the pulse
1	0.00023	True	False	246.0868	
1	0.00023	True	False	246.0873	

The table FP Time and DAS FP Time then need to be aligned together. First, the longer data set, in this case DAS FP Time, is trimmed such that both data sets have the same length. Second, a function of the FP Time relation is calculated using a linear polynomial. This function is then used to transfer Table Time to DAS Time.

Even though both data sets are now aligned at the start of the freeze pulse after the recording trigger was activated, they are of different length. Additionally, they are in a different time interval due to

<sup>4</sup>according to the documentation, the first recorded pulse took place at time  $n - 1$

<sup>5</sup>one pulse period consist of 20 samples: 10 True and 10 False

the particular clock rate. To match the data, first they both are modified into a time series format, where each data set is paired up with their respective clock time. Then using the MATLAB<sup>®</sup> *synchronize* function, the two time series are re-sampled using a common time vector and a specified method. In this case, the *Uniform* method is chosen because the exact interval can be specified.

### 3.3 Test Set-up with External Signal

The purpose of the test set-up shown is to compare the Table and DAS behaviour in sampling the same signal. Timing evaluation and signal quality in both acquisition systems will determine not only the measured signal characteristics, but also the synchronization validity. Figure 5 shows the test setup diagram, which instead of measuring the angular accelerometer and the calibration table output, it measure a common signal. The input signal is generated by an external signal generator to ensure its stability. The DAS sent the sync pulse continuously to the Table's controller, since the the beginning of the measurement. The log active trigger was sent from the DAS computer to the Table's controller, to start logging/ recording the measurement.

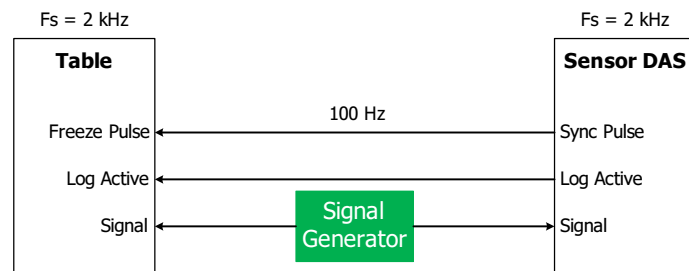


**Figure 5: Test set-up with sync pulse and external signal**

Besides static measurements, the test also incorporates a configuration that can simulate dynamic measurements. Two motion profiles are applied to the turn-table: a 30 deg/s constant rate and a single frequency sinusoidal. Also, the sync pulse is varied at a 100 Hz and 500 Hz rate to examine whether a higher rate pulse can improve the synchronization accuracy.

## 4 TEST RESULTS

The test setup configuration test plan explained in Section 3.3 is summarized in Table 2. In the experiment, the generated external signal  $S$  is measured in the calibration table as  $S_{tab}$ , and in the sensor DAS as  $S_{das}$ . Afterwards, the measured data sets are subject to the synchronization procedures in Section 3.2 on page 5. Subsequently, synchronization evaluation is performed based on three criteria: signals delay, clocks stability, and clocks relation in synchronization.

FP Rate (Hz)	Motion Profile	Signal
100	Static	8 volts continuous sinusoidal at 1 Hz
	Constant Rate 30 deg/s	
	Sinusoid	
500	Static	
	Constant Rate 30 deg/s	
	Sinusoid	

**Table 2: Test setup measurement plan.**

#### 1. Signal input

The recorded analog signal in the control center and sensor DAS, before the synchronization, are shown in the first row of Figure 6 on the next page. Based on their PSD in the second row, they



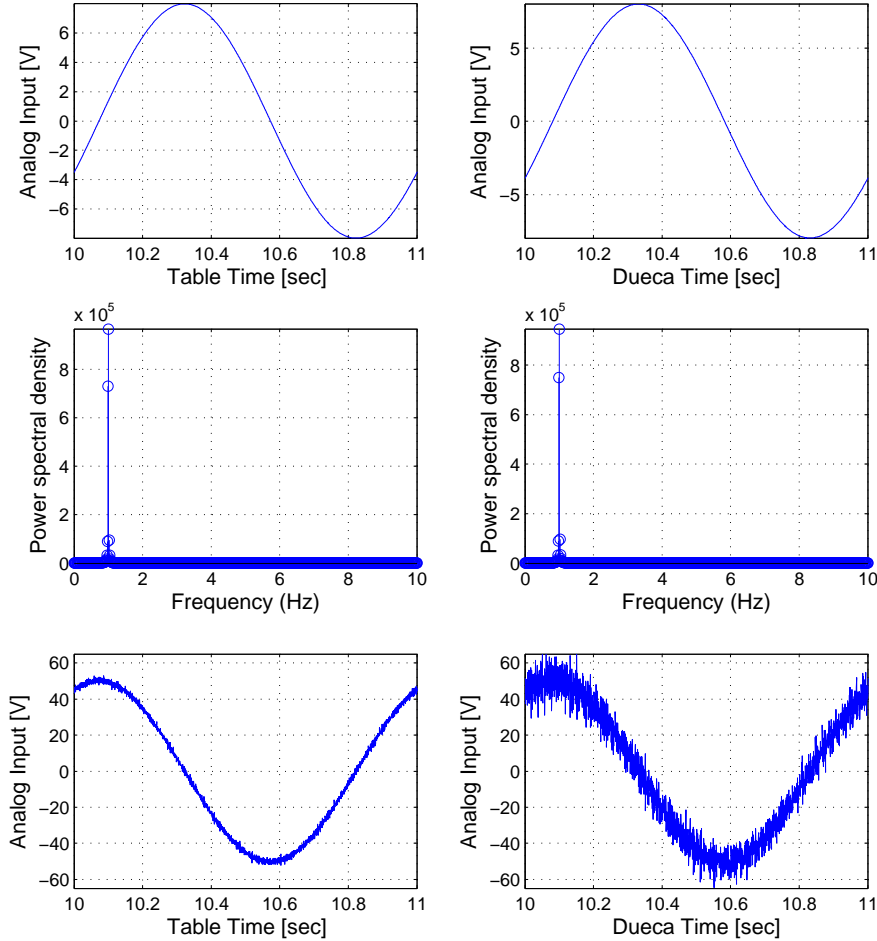


**Figure 6:** Measured signal in the calibration table and sensor DAS

represent clean signals. However, their respective 1<sup>st</sup> order derivatives which are presented in the third row of the same figure, shows that sensor DAS signal derivative has a higher noise level.

## 2. Comparison with an Ideal Signal

The measured signals are compared with an ideal, simulated signal  $S_I$  of the same amplitude and frequency as presented in Figure 7 on the following page. There are delay present between  $S_I$  and the synchronized data, then assessed individually:

$$\Delta S_{tab} = S_I - S_{tab} = 158$$

$$\Delta S_{tab} = S_I - S_{das} = 158$$

The identical delays indicate that both  $S_{tab}$  and  $S_{das}$  have equivalent orientation towards  $S_I$ . Hence, it can be said that the proper synchronization procedures has been applied to align the signals.

## 3. Timing Evaluation

Jitter is the timing variation of a set of signal edges from their ideal values, which in clock signals

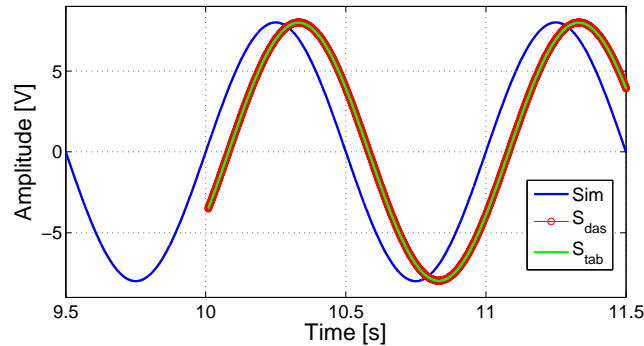
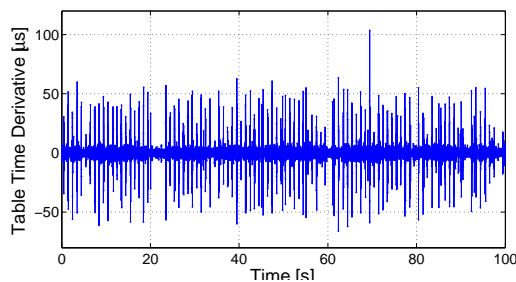


**Figure 7:** Comparison of measured and simulated sinusoidal signal

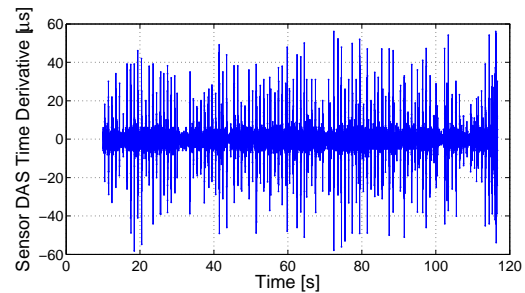
are typically caused by noise or other disturbances in the system. Figure 8 shows the calibration table and sensor DAS jitter in the form of 1<sup>st</sup> order derivatives of the clock. Since all known signals contain jitter that has a random component, statistical measures are required to properly characterize the jitter. Table 3 present some of the commonly used measures. The histogram in Figure 9 on the next page shows that both jitters approximately has a Gaussian distribution with standard deviation of  $8.5\mu s$  and  $7.13\mu s$ .

**Table 3: Jitter statistical measures.**

Measures	Calibration Table	Sensor DAS
Mean [ $\mu s$ ]	9998.75	10000
Standard Deviation [ $\mu s$ ]	8.5	7.13
RMS [ns]	9.999	10



(a) Table time jitter



(b) Sensor DAS time jitter

**Figure 8: Table Time and DAS Time jitter**

#### 4. Clock relation in synchronization

After the synchronization procedure in Section 3.2 on page 5, the identified Table and DAS time relation are subject to a linear approximation of the curve to map their relation and presented in Figure 10 on the next page, along with the residual. Figure 11 on page 12 presents the plot of the synchronized calibration table and angular accelerometer data that is perfectly aligned. Nevertheless, the residual or error still contains an oscillation which is shown by two small frequency components at  $1Hz$  and  $50Hz$  in Figure 11(c) on page 12.

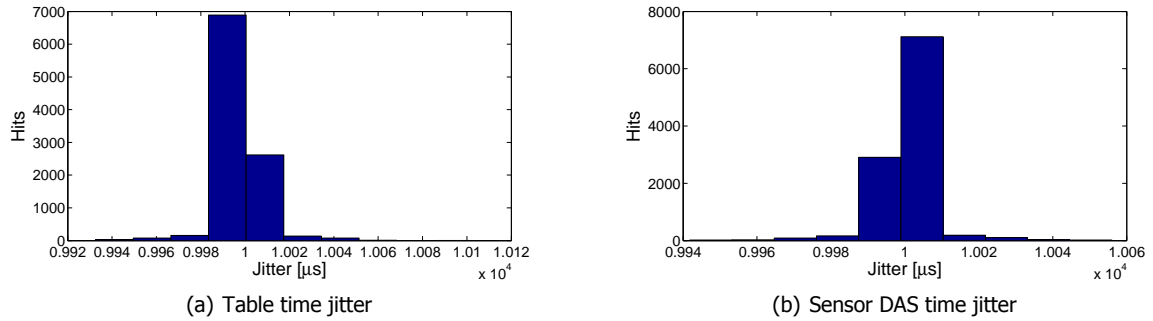


**Figure 9: Table Time and DAS Time jitter histogram**

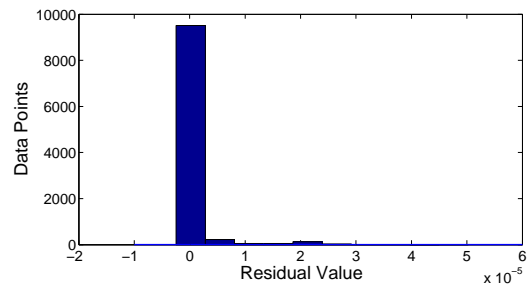
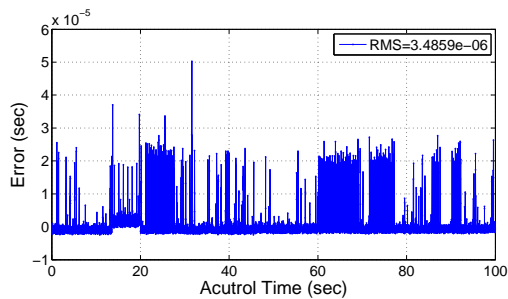
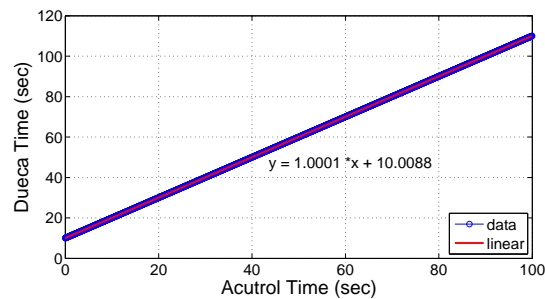
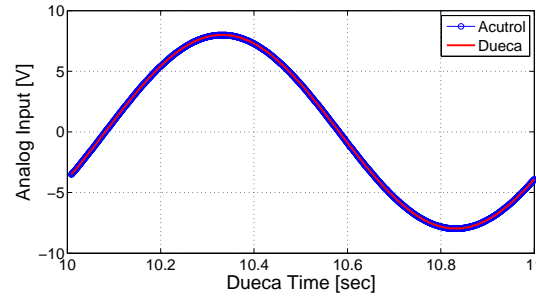
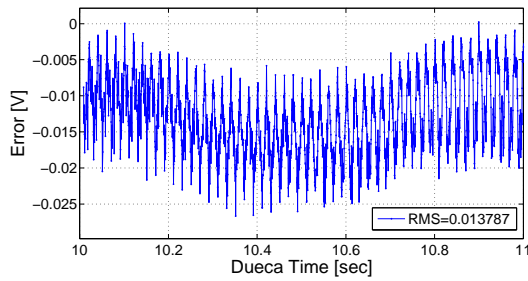


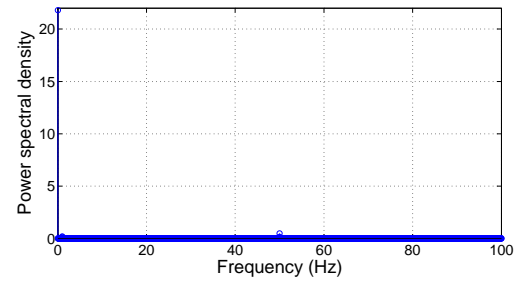
**Figure 10: Acutrol Time vs Dueca Time with Linear Fit and Residual at Static**



(a) Synchronized and resampled datasets



(b) Residual



(c) Residual PSD

**Figure 11:** Synchronized and resampled datasets at Static, with residual and its PSD.

The previous example is from the static measurement with a  $100\text{Hz}$  freeze pulse. Table 4 presents the summary of clock relation error RMS, sync-ed signals error RMS, and sync-ed signals delay, from all three applied profiles and two different freeze pulse frequencies.

**Table 4:** Comparison.

Item Description		Clock relation error RMS (s)	Sync-ed signals error RMS (V)	Sync-ed signals delay (sample)
100 Hz	Static	3.486e-06	13.787e-03	0
	Constant Rate	2.861e-06	12.76e-03	0
	Sine	3.086e-06	12.412e-03	0
500 Hz	Static	3.079e-06	12.505e-03	0
	Constant Rate	3.546e-06	12.474e-03	0
	Sine	3.058e-06	12.495e-03	0

The error in the RMS value can be calculated using the following equation:

$$Error_{RMS} = \frac{\sigma_n}{\sqrt{2N}} \quad (2)$$

Where  $\sigma_n$  is the RMS or standard deviation of the collected sample and  $N$  is the sample size. In this case, the sample size is  $2^{17}$  or 131,072. Accordingly,  $Error_{RMS}$  is  $0.00195\sigma_n$ . The Gaussian probability density function (PDF) for this number of sample as specified by the JEDEC standard<sup>6</sup> is  $\pm 5.672$ . Therefore, the clock relation RMS and sync-ed signals error RMS are all fall below the mentioned limit. Having considered this, it is reasonable to consider that the proposed synchronization procedures is acceptable for the customized setup.

<sup>6</sup>www.jedec.org

## 5 CONCLUDING REMARKS

An accurate angular acceleration reference is an absolute necessity in angular accelerometer dynamic calibration. Since an angular accelerometer is not yet used in standard equipment of an aircraft, little attention has been given to its calibration in an inertial frame arrangement. Such a calibration procedure is common for gyroscope, utilizing a turn-table to precisely reproduce aircraft motion in three body-axis: pitch, roll and yaw. Therefore, the widely available equipment performance is proven for a gyroscope's angular velocity, but not to angular accelerometer's angular acceleration.

Several issues arise in current sensor calibration system. Most prominently, angular accelerometer noise levels exceed the specification when using the basic slip-rings set-up. The possible solution on how to carry out the angular accelerometers calibration experiment has been presented in this paper. It comprise establishing a new, customized set-up for angular acceleration calibration. This approach addresses the dynamic angular calibration challenges for angular accelerometers. In the customized setup, sensor DAS connects directly to the angular accelerometer data channels and in this way, resulting in a lower noise level within the sensor specification. A test setup measuring a common signal generated by a stable pulse generator is used to check the setup noise. With the proposed set-up and scheme, users are able to utilize the currently available position based-calibration table in the dynamic angular accelerometer calibration.

## Acknowledgments

The authors would like to thank F. Postema and H. Thung from the Control and Simulation Section, Faculty of Aerospace Engineering – Delft University of Technology, who provide their exceptional assistance in establishing the customized angular accelerometer measurement set-up.

## References

- [1] Gyro and Accelerometer Panel, "IEEE Standard Specification Format Guide and Test Procedure for Non-gyroscopic Inertial Angular Sensors Jerk, Acceleration, Velocity, and Displacement," Std 671-1985, IEEE Aerospace and Electronic Systems Society, New York, NY, 1985.
- [2] DeMore, L. A., Mackin, P. R., Swamp, M., and Rusterholtz, R., "Improvements in Flight Table Dynamic Transparency for Hardware-in-the-loop Facilities," Proceedings of SPIE 4027, Technologies for Synthetic Environments: Hardware-in-the-Loop Testing V, SPIE, 2000, pp. 101–112.
- [3] Peters, R. B., "A Dynamic Angular Calibration System for Broadband Microradian Inertial Sensors," AIAA, 1978, pp. 541–550.
- [4] Sieberling, S., Chu, Q. P., and Mulder, J. A., "Robust Flight Control Using Incremental Nonlinear Dynamic Inversion and Angular Acceleration Prediction," Journal of Guidance, Control, and Dynamics, Vol. 33, No. 6, 2010, pp. 1732–1742.
- [5] Falkena, W., Borst, C., van Oort, E. R., and Chu, Q. P., "Sensor-Based Backstepping," Journal of Guidance, Control, and Dynamics, Vol. 36, No. 2, 2013, pp. 606–610.
- [6] Sun, L. G., de Visser, C. C., Chu, Q. P., and Falkena, W., "Hybrid Sensor-Based Backstepping Control Approach with Its Application to Fault-Tolerant Flight Control," Journal of Guidance, Control, and Dynamics, Vol. 37, No. 1, 2014, pp. 59–71.
- [7] Ovaska, S. J. and Valiiviita, S., "Angular Acceleration Measurement: A Review," Proceedings of IEEE Instrumentation and Measurement Technology Conference, IEEE, 1998, pp. 875–880.
- [8] Merhav, S., Aerospace Sensor Systems and Application, Springer, 1996.

- [9] Meydan, T., "The Development of Accelerometers Technology," *Sensors and Actuators A: Physical*, Vol. 59, No. 2, 1997, pp. 43–50.
- [10] Gyro and Accelerometer Panel, "IEEE Standard Specification Format Guide and Test Procedures for Linear Single-Axis, Nongyroscopic Accelerometers," Std 1293-1998, IEEE Aerospace and Electronic Systems Society, 1998.
- [11] Kamer, Y. and Ikizoglu, S., "Measurement of Angular Accelerations, Angular Velocities and Rotation Angles by Grating Interferometry," *Elsevier – Measurement*, Vol. 46, 2013, pp. 1641–1649.
- [12] Dube, D. and Cardou, P., "The Calibration of an Array of Accelerometers," *Transactions of the Canadian Society for Mechanical Engineering*, Vol. 35, 2011, pp. 251–267.
- [13] Zheng, Z. Y., Gao, Y. B., and He, K. P., "Systematic Calibration Method for FOG Inertial Measurement Units," *Advanced Materials Research*, Vol. 662, 2013, pp. 717–720.
- [14] Xie, B., Qin, Y., and Wan, Y., "A High Accuracy Calibration Method of Optical Gyro SINS," *IEEE*, 2010, pp. 507–511.
- [15] Sun, W., Wang, D., Xu, L., and Xu, L., "MEMS-based Rotary Strapdown Inertial Navigation System," *Elsevier – Measurement*, Vol. 46, 2013, pp. 2585–2596.
- [16] de Oliveira, E. J., de Castro Leite Filho, W., and da Fonseca, I. M., "Inertial Measurement Unit Calibration Procedure for a Redundant Tetrahedral Gyro Configuration with Wavelet Denoising," *Journal of Aerospace Technology and Management*, Vol. 4, 2012, pp. 163–168.
- [17] Nieminen, T., Kangas, J., Suuriniemi, S., and Kettunen, L., "An Enhanced Multi-Position Calibration Method for Consumer-Grade Inertial Measurement Units Applied and Tested," *Measurement Science and Technology*, Vol. 21, No. 10, 2010, pp. 11.
- [18] Lamport, L., "Time, Clocks, and the Ordering of Events in a Distributed System," *Communications of the ACM*, Vol. 21, No. 7, 1978, pp. 558–565.